Unveiling a Complex Phase Transition in Monolayers of a Phospholipid from the Annular Region of Transmembrane Proteins

Òscar Domènech,[§] Jordi Ignés-Mullol,[§] M. Teresa Montero,[‡] and Jordi Hernandez-Borrell*[,‡]

Departament de Química Física, Facultat de Química, and Departament de Fisicoquímica, Facultat de Farmàcia, Universitat de Barcelona, E-08028 Barcelona, Spain

Received: March 16, 2007; In Final Form: June 21, 2007

The lateral packing properties of phospholipids that surround transmembrane proteins are fundamental in the biological activity of these proteins. In this work, Langmuir monolayers of one such lipid, 1-palmitoyl-2-oleoyl-*sn*-glycero-3-phosphoethanolamine (POPE), are studied with a combination of pressure−area isotherm analysis, Brewster angle microscopy, and atomic force microscopy of extracted films. The analysis reveals a sequence of phase transitions LE−LC−LC′ occurring in a narrow packing range. The lateral pressures and area densities of these phases provided meanings for the packing requirements in the annular lipid region of typical transmembrane proteins.

Introduction

The physicochemical influence of the surrounding lipid bilayer on transmembrane proteins (TMPs) is poorly understood at the molecular level. The physiological activity of the TMPs may be influenced by or dependent on the physical properties of neighboring phospholipids.[1] Such dependence has been demonstrated for several TMPs, e.g., β-hydroxybutyrate dehydrogenase, an enzyme integrated into the mitochondrial inner membrane; the ion pump Ca^{+2}-ATPase,[2] melibiose permease,[3] and lactose permease (LacY)[4] of *Escherichia coli* (*E. coli*); and the homotetrameric potassium channel KcsA of *Streptomyces lividans*.[5] On the other hand, the membrane phospholipids where the TMPs are embedded include mixed acyl chains (one saturated, the other unsaturated at the *sn*-2 position) linked to the glycerol backbone. Such is the case with 1-palmitoyl-2-oleoyl-*sn*-glycero-3-phosphoethanolamine (POPE). This particular phospholipid plays a crucial role for active transport in the LacY[6] system. Besides, POPE acts as a chaperone for the in vivo assembly of LacY and folding of the epitope for a monoclonal antibody.[7,8] Suggesting a more general involvement of these phospholipids in the structure and activity of TMPs, POPE has been shown to be important for the efficient membrane association and tetramerization of KcsA.[5] To produce such effects, the phospholipids in the immediate vicinity (the so-called annular lipid region) of the TMPs should be molecules that may easily adapt to the highly irregular surfaces of the integral proteins.[9] In this regard, the packing properties of the phospholipids, particularly their ability to provide the lateral force for an adequate stress profile,[10] becomes of relevance in the biological context. To accomplish such physicochemical requirements, the annular phospholipids should be highly compressible, in fluid phase and with a definite shape in order to provide an adequate thickness to match the hydrophobic membrane-spanning region of the TMPs.[11] It is within this biological context that the interfacial properties of POPE become relevant.

When in suspension in an excess of water, POPE shows two well-characterized thermal transitions: (i) the solid-crystalline (L_β) to the liquid-crystalline (L_α) at ∼24 °C, also known as the gel- to liquid-phase transition temperature (T_m); and (ii) the lamellar to inverted hexagonal (H_{II}) phase transition at elevated temperatures, ∼80 °C (T_H). As a consequence of its tendency to form H_{II} phases, it is believed that POPE may provide, in specific conditions, the adequate curvature to the membranes.[12,13]

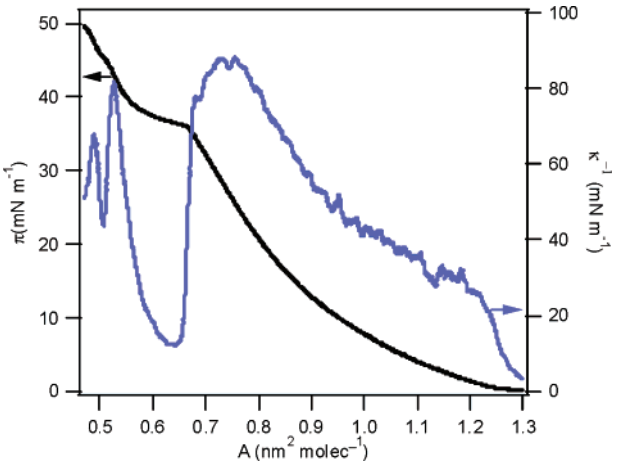

Figure 1. $\pi-A$ isotherm and compressibility modulus (κ) of the POPE monolayer at 24 °C.

On the other hand, POPE monolayers at the air−water interface are in liquid expanded (LE) phase up to 36.0 mN m^{-1}, where they exhibit a characteristic transition toward a liquid condensed (LC) phase. Actually, judging the different published isotherms,[14,15] a certain controversy appears in the interpretation of the nonhorizontal plateau where this transition occurs. The morphology of the monolayer isotherm ressembles the typical LE−LC phase transition,[15] but data published for a monolayer of OPPE[16] (the structural isomer of POPE) point to a transition between two liquid condensed phases (namely, LC and LC′).[17]

The present study was designed to characterize, at micrometer and nanometer scale and by means of Brewster angle microscocpy (BAM) and atomic force microscopy (AFM) techniques, POPE monolayers and, in particular, to visualize, by means of these techniques, the distinctive phase transition occurring within the plateau region. We are able to characterize

* Corresponding author. E-mail: jordihernandezborrell@ub.edu.
§ Departament de Química Física, Facultat de Química.
‡ Departament de Fisicoquímica, Facultat de Farmàcia.

10.1021/jp0721144 CCC: $37.00
Published on Web 08/24/2007

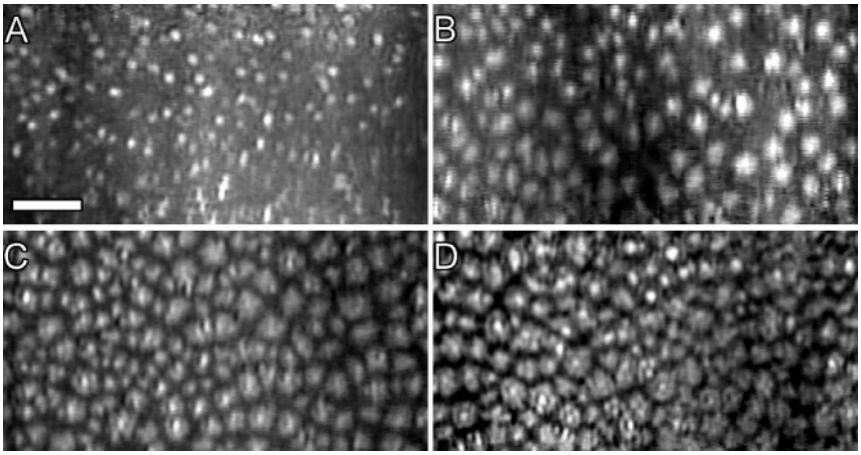

Figure 2. BAM images at $T = 24$ °C and 15 (A), 36 (B), 38 (C), and 39 mN·m^{-1} (D). The bar represents 100 μm.

the nature of the phase transition taking place within the plateau region and reveal a new transition at a high lateral pressure.

Experimental Section

1-Palmitoyl-2-oleoyl-*sn*-glycero-3-phosphoethanolamine, specified as 99% pure, was purchased from Avanti Polar Lipids (Alabaster, AL). The subphase buffer beneath the monolayers was a 50 mM Tris·HCl buffer (pH 7.40) containing 150 mM NaCl, prepared in Ultrapure water (Milli Q reverse osmosis system, 18.3 MΩ·cm resistivity). Chloroform and methanol, HPLC grade, were purchased from SIGMA (St. Louis, MO).

Surface Pressure−Area Isotherms. The preparation of the monolayers was performed in a 312 DMC Langmuir−Blodgett trough manufactured by NIMA Technology Ltd. (Coventry, England). The trough (total area, 137 cm^2) was placed on a vibration-isolated table (Newport, Irvine, CA) and enclosed in an environmental chamber. The resolution of the surface pressure measurement was ±0.1 mN·m^{-1}. In all experiments the temperature was maintained at 24.0 ± 0.2 °C via an external circulating water bath. Before each experiment, the trough was washed with chloroform and rinsed thoroughly with purified water. The cleanliness of the trough and subphase was ensured before each run by cycling the full range of the trough area and aspirating the air−water surface, while at the minimal surface area, to zero surface pressure.

The experiments were carried out as described in previous papers.[14,17] The lipid was dissolved in chloroform−methanol (3:1, v/v) to a final concentration of 1 mg·mL^{-1}. The corresponding aliquot of lipid was spread onto the surface of the subphase solution with a Hamilton microsyringe. A 15 min period was required to allow the solvent to evaporate before each experiment. The compression barrier speed was 5 cm^2·min^{-1}. Every surface pressure−area (π−A) isotherm was repeated three times minimum, with the isotherms showing satisfactory reproducibility. The surface compressibility modulus (κ) of the monolayer was calculated from isotherms using $\kappa = (-1/A)(\partial A/\partial \pi)_{T,n}$.[18] The derivative of the experimental data was determined by fitting a straight line to a window of 40 data points around any given value, so that experimental noise is filtered out. LB films for AFM observations were transferred onto freshly cleaved mica, lifting the substrate at a constant rate of 1 mm·min^{-1}. The transfer ratios were evaluated and proved near unity, indicating that the mica was almost fully covered with the monolayer.

Brewster Angle Microscopy. A custom-built Brewster angle microscope,[19,20] based on a polarizing reflection microscope,

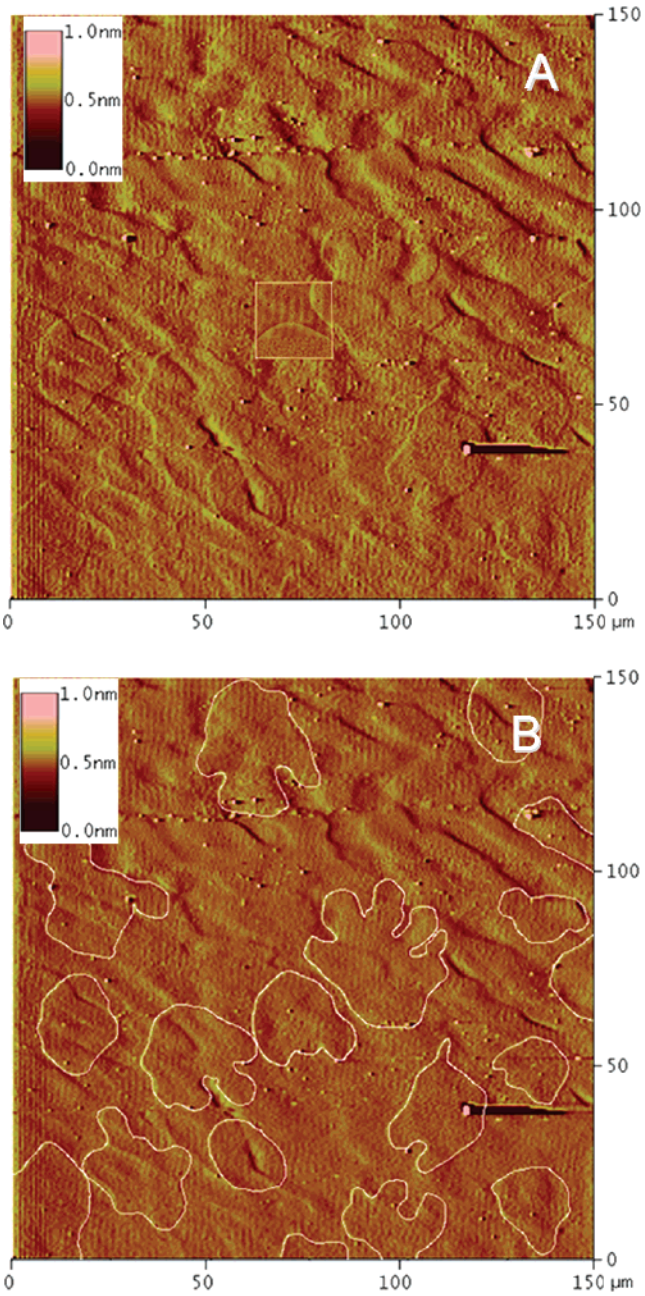

Figure 3. Deflection AFM image of Langmuir−Blodgett film of POPE extracted at 39 mN·m^{-1} and $T = 24$ °C (A). Features have been highlighted (B) by marking the contour in white as a guide to the eye to evidence its resemblance with LC domains in Figure 2D. The white square region in A has been magnified, and it is shown in Figure 4D.

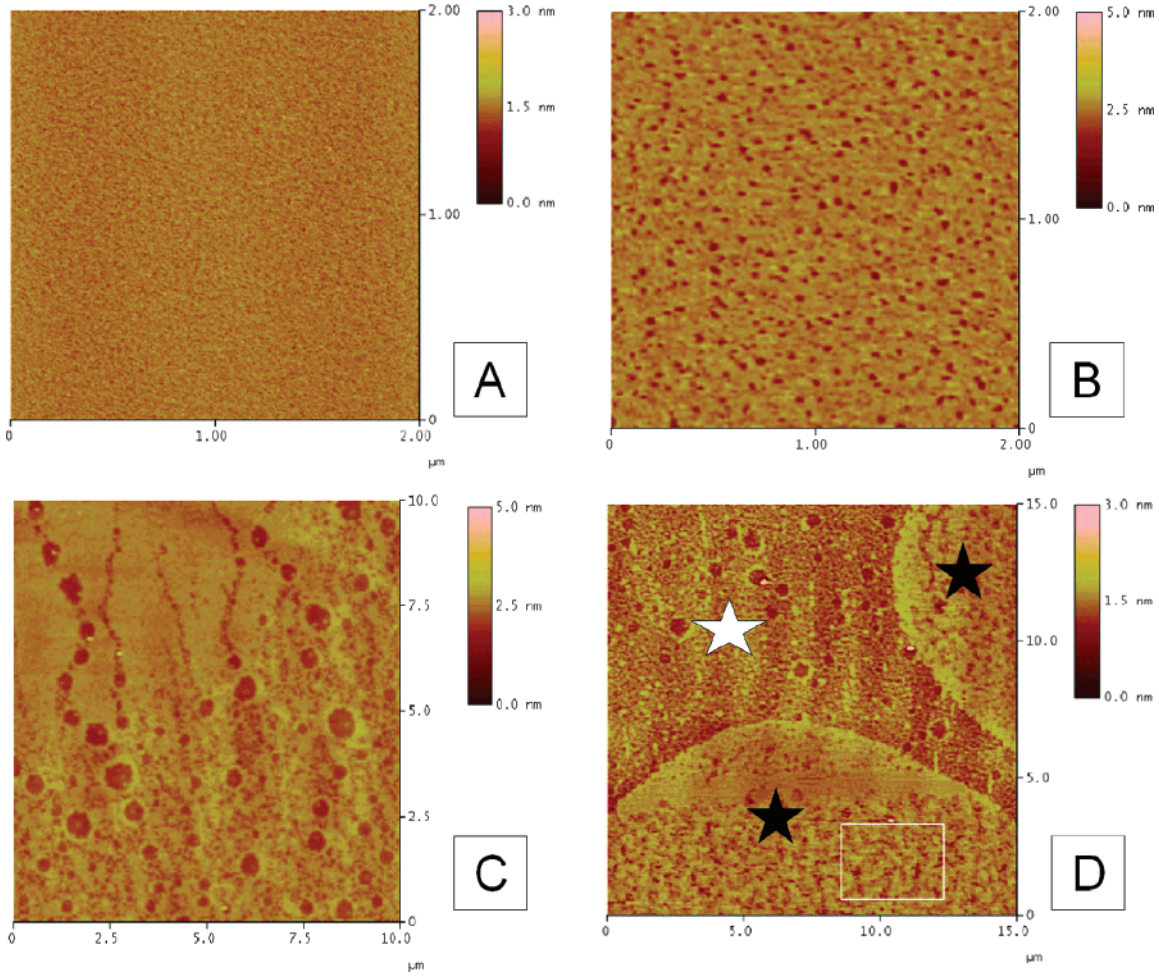

Figure 4. AFM topographic images POPE LB films extracted at $T = 24$ °C: LB films at 10 (A), 30 (B), 36 (C), and 39 mN·m^{-1} (D).

is used to monitor in real time the configuration of the Langmuir monolayers at the mesoscale.

The instrument is equipped with a collimated 30 mW red diode laser ($\lambda = 690$ nm, Monocrom S.L., Spain) linearly polarized in the plane of incidence by a Glann-Thomson polarizer. The reflection from the interface passes through a second Glann-Thomson polarizer and is picked by an IR-enhanced CCD camera (JAI-CV-M50IR). Images are recorded in DVD format, and further digital image processing is performed with the public domain software ImageJ.[21]

The microscope is adjusted so that reflection from the bare air−water interface is minimal. As a result, it is sensitive to local changes in the optical properties of the interface.[22] This is particularly useful for studying monolayer phase transitions since one can discern among changes in packing density, long-range ordering, or film thickness between coexisting phases.[23]

Atomic Force Microscopy. AFM measurements were made at a constant temperature of 24 °C with a Nanoscope III from Digital Instruments, Santa Barbara, CA, equipped with a 150 μm piezoelectric scanner. Details of the experiments have been given elsewhere.[17] Briefly, the images were taken in air in contact mode with a silicon cantilever and a nominal spring constant of 40 pN·nm^{-1}. The applied force was kept as low as possible to minimize monolayer damaging. Roughness was calculated in different spots of the images over areas of 2 μm^2. All the images were processed using Digital Instruments (Nanoscope 6.12r1) software.

Results and Discussion

The $\pi-A$ isotherm of the POPE monolayer at 24.0 ± 0.2 °C is shown in Figure 1. The pressure increases steadily at areas below 1.4 nm^2·molecule^{-1} until 36.0 mN·m^{-1}, where a plateau extends from ∼0.68 to ∼0.57 nm^2·molecule^{-1}, while π increases by approximately 2 mN·m^{-1}. Finally, the monolayer collapses at 50.7 mN·m^{-1}. These features are in basic agreement with previously published data.[24,25] A sequence of BAM images at 15, 36, 38, and 39 mN·m^{-1} are shown respectively in Figure 2A−D. For areas above 1.4 nm^2·molecule^{-1}, π is negligibly small and images show the coexistence between the gas and LE phases (image not shown).

While the isotherms in the LE phase are featureless, BAM images reveal the nucleation of bright spots (Figure 2A). Their number does not appear to increase above $\pi \sim 6$ mN·m^{-1}, although they become increasingly brighter upon compression. They are roughly 5 μm in diameter, although this size is near the resolution of our BAM images. Images do not reveal any new emerging structures until the plateau region. There, growth of lobulated domains with increased BAM reflectivity is observed (Figure 2B,C) consistent with a LE−LC phase transition. Bright spots present at lower pressures act as nucleation points of the new domains, whose structure is typical in condensing LC domains in phospholipid monolayers.[26] It is also interesting to notice that there is a subtle slope change in the isotherm at 45 mN·m^{-1} (see Figure 1) that had not been reported in previous works.[15,24−27] This feature was reproducible under the experimental conditions of this work. The contrast in

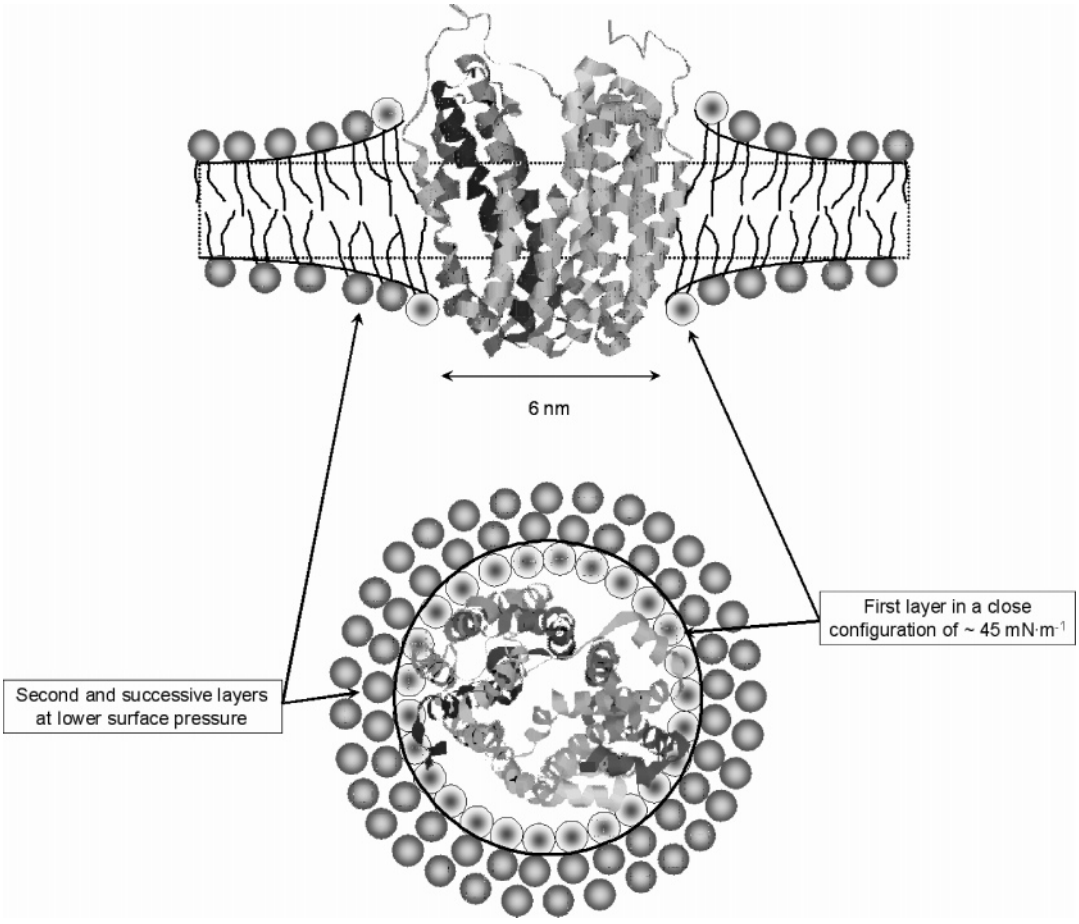

Figure 5. Tentative model for the annular phospholipid distribution of POPE molecules around the transmembrane protein lactose permease (LacY) of *Escherichia coli* (6 nm of diameter). The first shell would be constituted by ∼26 molecules whose average area (0.52 $nm^2 \cdot molecule^{-1}$) has been estimated from the POPE isotherm at a surface pressure of 45 $mN \cdot m^{-1}$. The second shell would be constituted by molecules at lower surface pressures (30 $mN \cdot m^{-1}$). Notice that the cross-section of the PE pressures as high as those considered here are given by the area of the aliphatic tails.[33]

the BAM images is too small at this high lateral pressure to be able to distinguish any changes in the mesoscopic structure. However, absence of new bright spots (which would imply the onset of monolayer collapse) suggests that there is a transition into a different condensed phase.

To get further insight into the molecular ordering of the monolayer, AFM was used to complement our BAM observations. First of all, as proof of concept, a large AFM deflection image of a LB film extracted at 39 $mN \cdot m^{-1}$ is presented in Figure 3A to allow the comparison at similar scales with the BAM image at 39 $mN \cdot m^{-1}$ (Figure 2D). Condensed domains in BAM images present sizes and shapes (highlighted in white in Figure 3B) remarkably similar to the polygonal motifs observed by AFM, suggesting that the LB transfer preserves the structure at the air−water interface. A sequence of AFM images extracted at surface pressures of 10, 30, 36, and 39 $mN \cdot m^{-1}$ are shown in Figure 4A−D, respectively. The LB extracted at 10 $mN \cdot m^{-1}$ (Figure 4A) was featureless, as expected for a region where only one phase (LE) exists. The topography, with an average surface roughness, $R_a \sim 0.05$ nm, appears smoother than others found in the literature for POPE at a similar surface pressure.[15] At 30 $mN \cdot m^{-1}$ numerous randomly distributed vacancies, with a mean diameter of ∼75 nm, are observed (Figure 4B). As pressure increases these vacancies coalesce resulting in regions with diameter ranging from ∼90 to ∼500 nm at 36 $mN \cdot m^{-1}$ (Figure 4C). In turn, R_a increases from 0.14 to 0.18 nm with this surface pressure raise. The origin of these vacancies is somewhat intriguing. On the one hand, it can be shown that small variations in the transfer ratio of the LBs onto mica result in the desorption of phospholipid molecules.[28] On the other hand, depths between 0.80 and 1.16 nm can be measured for the vacancies observed in Figure 4B,C, clearly lower than the thickness expected for a phospholipid monolayer. Indeed, recent force spectroscopy analysis provided evidence that depth measurements based on AFM topography images could erroneously lead to the conclusion that the vacancies found in LBs of POPE are intrinsic features of this monolayer.[29] Furthermore, these vacancies grow within much more complex structures, as observed at 39 $mN \cdot m^{-1}$ (Figure 4D). This image (a magnification of the highlighted white square in Figure 3A) shows two well-defined domains with a step-height difference of ∼0.5 nm. This is a typical difference between LC and LE phases.[30] Hence, while the lower domain (white star) would represent the LE phase, the upper domain (black star) would represent the LC phase. In the work of Saulnier et al.,[15] however, it was proposed that the LE−LC phase transition of POPE occurred by nucleation of microdomains that are, indeed, similar to those that we observed in the upper domains (see white square highligthed in Figure 4D). Although we agree that a nucleation process occurs, as evidenced by our BAM observations, we believe that these authors were observing regions within the large lobulated domains shown in parts D and C of Figure 2.

Earlier works by Rey-Gómez-Serranillos et al.[16] with OPPE (the structural isomer of POPE) reported a plateau in the isotherms at a lateral pressure $\pi = 38.5$ $mN \cdot m^{-1}$. On the basis of BAM imaging and analysis of the isothermal compressibility,

κ^{-1}, these authors suggest that there is evidence of a transition between two condensed phases (LC−LC′) rather than the condensation of a LE phase. Transitions between condensed phases are typical in mesophases of long-chain fatty acids that differ either in the arrangement of the hexatic lattice, molecular tilt-bond orientational order or molecular backbone symmetry.[31,32] In an earlier work,[14] we considered that the plateau region in POPE isotherms is consistent with a LC−LC′ transition, in analogy with published work with OPPE. We will argue now that the data reported here suggest a revision of such an interpretation. Moreover, we will propose that there is evidence of a LC−LC′ transition at pressures above the plateau region.

One of the central arguments in the work with OPPE monolayers resided in the bimodal nature of κ^{-1} vs π. We evaluated here this relationship from the POPE isotherm at 24 °C (see Figure 1). A steep drop in κ^{-1} occurs within the plateau region, being the relative maxima 90 and 80 mN·m^{-1}, before and after the transition, respectively. These values are comparable to those reported for OPPE monolayers, 85 and 75 mN·m^{-1} (subphase was water with pH 6 in that work). Although this behavior was taken as evidence for a LC−LC′ transition in OPPE, our BAM observations suggest that the plateau region corresponds to a LE−LC phase transition. In fact using the analysis of κ^{-1} as the only evidence of a LC−LC′ phase transition is prone to suffer from numerical artifacts derived from the method used to obtain the compressibility from derivatives of the experimental data. The use of qualitative AFM imaging (Figure 4) shows the coexistence of two phases in the plateau region but cannot give a conclusive answer for the nature of such phases.

One relevant finding of our work, however, is the evidence for a second transition in the POPE monolayers. A kink in the isotherm can be observed around 45 mN·m^{-1}, which results in the formation of a maximum in κ^{-1} of about 65 mN·m^{-1}. At these high lateral pressures, the BAM image contrast is too low to observe changes in the mesoscopic ordering consistent with a LC−LC′ phase transition. Besides, at this pressure, desorption of the molecules during the LB extraction occurs and AFM images could not be obtained. Nevertheless, we believe that the evidence from thermodynamic data is enough to prove the presence of this new condensed phase. In any case, the true nature of condensed phases should only be unambiguously assessed by means of X-ray diffraction techniques.[33]

In summary, on the basis of the combination of thermodynamic, BAM imaging, and AFM imaging data, we conclude that the complex scenario undergone by POPE monolayers includes a LE−LC transition, beginning at the plateau region and ending at the second transition point (i.e., 26 and 45 mN·m^{-1} at 24 °C), where a new condensed phase (LC′) would precede the collapse of the monolayer.

Numerous evidence pointed to the fact that the PE group provides a better surface interaction with TMPs than other species.[10,34] Indeed, PE represents about 82 wt % of the inner cytoplasmic membrane of *E. coli*,[35] where LacY is embedded. To stress the importance of lateral compressibility as a crucial physical parameter involved in phospholipid−protein membrane interactions, it is illustrative to perform a rough estimation of the lipid requirement for a single TMP model at two pressures. For LacY, for instance (Figure 5), we can assume a diameter of 6 nm[36] and by taking the molecular areas of the POPE monolayer at 30 and 45 mN·m^{-1} (0.72 and 0.52 nm^2·molecules^{-1}, respectively) a simple calculation yields that 26 or 28 molecules of POPE might constitute, at 30 and 45 mN·m^{-1} surface pressures, the first shell of the annular region of the protein. Normally, 30 mN·m^{-1} is often assimilated to the lateral surface pressure of the biological membranes,[37,38] but it is reasonable to assume that higher pressures up to 45 mN·m^{-1} could be reached in the vicinity of TMPs. It is true that similar values could be achieved for other phospholipids, such as DPPC (in LC phase at these surface pressures) or POPC (always in LE phase). However, the important feature of POPE resides, considering only nonspecific interactions,[39] on its ability to undergo the LE to LC, eventually LC′, phase transition within the range of surface pressures of biological membranes that undoubtedlty are relevant in our understanding of lipid−protein interactions in biomembranes.

Acknowledgment. Ò.D. was recipient of a "Recerca i Docència" fellowship from the University of Barcelona. J.I.-M. is recipient of a "Ramon y Cajal" fellowship from the Ministerio de Ciencia y Tecnologia (MCYT). This work was supported by Grants CTQ2005-07989 and FIS2006-0352 from MCYT and SGR00664 (Generalitat de Catalunya) of Spain.

References and Notes

(1) Lee, A. G. *Biochim. Biophys. Acta* **2003**, *1612*, 1−40.
(2) Warren, G. B.; Toon, N. J. M.; Birdsall, A. G.; Lee, J. C.; Metcalfe, J. C. *Biochemistry* **1974**, *13*, 5501−5507.
(3) Dumas, F.; Tocanne, J. F.; Leblanc, G.; Lebrun, M. Ch. *Biochemistry* **2000**, *39*, 4846−4854.
(4) Le Coutre, J.; Narasimhan, L. R.; Patel, C. K. N.; Kaback, H. R. *Proc. Natl. Acad. Sci. U.S.A.* **1997**, *94*, 10167−10171.
(5) Valiyaveetil, F. I.; Zhou, Y.; Mackinnon, R. *Biochemistry* **2002**, *41*, 10771−10777.
(6) Seto-Young D.; Chen C C.; Wilson T H. *J. Membr. Biol.* **1985**, *84*, 259−267
(7) Bogdanov M.; Sun J.; Kaback. R.; Dowhan W. *J. Biol. Chem.* **1996**, *271*, 11615−11618.
(8) Bogdanov M.; Dowhan W. *J. Biol. Chem.* **1995**, *270*, 732−739.
(9) Fyfe, P. K.; McAuley, K. E.; Rozsak, A. W.; Isaacs, N. W.; Codgell, R. J.; Jones, M. R. *Trends Biochem. Sci.* **2001**, *26*, 106−112.
(10) Cantor, R. S. *J. Phys. Chem. B* **1997**, *101*, 1723−1725.
(11) Dumas, F.; Lebru, M. C.; Tocanne, J. F. *FEBS Lett.* **1999**, *485*, 271−277.
(12) Epand, R. M.; Bottega, R. *Biochim. Biophys. Acta* **1988**, *944*, 144−145.
(13) Rappolt, M.; Hickel, A.; Bringezu, F.; Lohner *Biophys. J.* **2003**, *84*, 3111.
(14) Domènech, Ò.; Torrent-Burgués, J.; Merino, S.; Sanz, F.; Montero, M. T.; Hernández-Borrell, J. *Colloids Surf., B* **2005**, *41*, 233−238.
(15) Saulnier, P.; Foussard, F.; Boury, F.; Proust, J. E. *J. Colloid Interface Sci*. **1999**, *218*, 40−46.
(16) Rey-Gómez-Serranillos, I.; Miñones, J., Jr.; Dynarowicz-Latka, P.; Miñones, J.; Conde, O. *Langmuir* **2004**, *20*, 11414−11421.
(17) Domènech, Ò.; Sanz, F.; Montero, M. T.; Hernández-Borrell, J. *Biochim. Biophys. Acta* **2006**, *1758*, 213−221.
(18) Petty, M. C. *Langmuir-Blodgett Films: An Introduction*; Cambridge University Press: New York, 1996.
(19) Hénon, S.; Méunier, J. *Rev. Sci. Instrum.* **1991**, *62*, 936−939.
(20) Hönig, D.; Möbius, D. *J. Phys. Chem.* **1991**, *95*, 4590−4592.
(21) Rasband, W. S. *ImageJ*; U.S. National Institutes of Health: Bethesda, MD, 1997−2007; http://rsh.info.nih.gov/ij.
(22) Meunier, J. *Colloids Surf., A* **2000**, *171*, 33−40.
(23) Fang, J. Y.; Teer, E.; Knobler, C. M.; Loh, K. K.; Rudnick, J. *Phys. Rev. E* **1997**, *56*, 1859.
(24) Mizuno, N. K.; Smaby, J. M.; Cunningham, B. A.; Monnsen, M. M.; Brockman, H. L. *Langmuir* **2003**, *19*, 1802−1808.
(25) Brokman, H. L.; Applegate, K. R.; Momsen, M. M.; King, W. C.; Glomset, J. A. *Biophys. J.* **2003**, *85*, 2384−2396.
(26) Weidemann, G.; Vollhardt, D. *Thin Solid Films* **1995**, *264*, 94−103.
(27) Raza Shaikh, S.; Brzustowicz, M. R.; Guftanson, N.; Stillwell, W.; Wassall, S. R. *Biochemistry* **2002**, *41*, 10593−10602.
(28) Bassereau, P.; Pincet, F. *Langmuir* **1997**, *13*, 7003−7007.
(29) Garcia-Manyes, S.; Domènech, Ò.; Sanz, F.;Montero, M. T.; Hernández-Borrell, J. *Biochim. Biophys. Acta* **2007**, *1768*, 913−922.
(30) Hollards, C. W.; Dunn, R. C. *Biophys. J.* **1998**, *75*, 342−353.

(31) Overbeck, G. A.; Möbius, D. *J. Phys. Chem.* **1993**, *97*, 1999−8004.
(32) Schwart, D. K.; Knobler, C. M. *J. Phys. Chem.* **1993**, *97*, 8849−8851.
(33) Kaganer, V. M. Möhwald, H.; Dutta, P. *Rev. Mod. Phys.* **1999**, *71*, 779−819.
(34) Bazzi, M. D.; Youakim, M. A.; Nelsesten, G. L. *Biochemistry* **1992**, *31*, 1125−1134.
(35) Merino-Montero, S.; Domènech, Ò.; Montero, M. T.; Hernández-Borrell, J. *Biophys. Chem.* **2005**, *118*, 114−119.
(36) Dowhan, W. *Annu. Rev. Biochem.* **1977**, *66*, 199−232.
(37) Blume, A. *Biochim. Biophys. Acta* **1979**, *557*, 32−44.
(38) Marsh, D. *Biochim. Biophys. Acta* **1996**, *1286*, 183−223.
(39) Bezrukov, S. M. *Curr. Opin. Colloid Interface Sci.* **2000**, *5*, 237−243.